

# A Data-Driven Multi-Residue Risk Classification Framework for Pesticide Contamination in Vegetables Using Hybrid Deep Learning

**Chaithra Reddy**

Presidency University, India

chaithra.20233cse0029@presidencyuniversity.in

**Joseph Michael Jerard**

Presidency University, India

josephmichaeljerard@presidencyuniversity.in (corresponding author)

Received: 15 January 2026 | Revised: 11 March 2026 and 30 March 2026 | Accepted: 1 April 2026

Licensed under a CC-BY 4.0 license | Copyright (c) by the authors | DOI: <https://doi.org/10.48084/etasr.17576>

## ABSTRACT

The increasing presence of pesticide residues in vegetables poses a major threat to public health, and there is an urgent need to develop efficient, accurate, and scalable detection methods. Traditional analytical techniques such as Gas Chromatography (GC) and Liquid Chromatography–Mass Spectrometry (LC–MS) offer high sensitivity but are expensive, labor-intensive, and unsuitable for large-scale or real-time screening applications. Recent advances in spectroscopy, machine vision, and Machine Learning (ML) show promise; however, most existing models rely on handcrafted or shallow features and fail to capture the complex spatial, textural, and thermal variations associated with multi-residue contamination. In this direction, the present study proposes a data-driven hybrid deep learning framework for multi-residue risk classification in vegetables using thermal imaging. This framework integrates  $\Delta T$ -based thermal image preprocessing, Gray-Level Co-occurrence Matrix (GLCM) texture descriptors, and deep feature embeddings extracted from InceptionV3, thereby forming a comprehensive hybrid feature vector. This fused representation is classified by a custom neural network trained with categorical focal loss to mitigate class imbalance and optimized using a cosine-decay learning rate to enhance convergence stability. Experimental evaluation on a custom thermal vegetable image dataset resulted in 84.97% validation accuracy and a loss of 0.0373, outperforming conventional Convolutional Neural Networks (CNNs) and other shallow classifiers. The model demonstrated good generalization with balanced precision and recall on contamination classes, supported by a well-converged training–validation performance and confusion matrix analysis. These results highlight the efficacy of this framework for non-destructive, real-time, and scalable pesticide contamination risk classification, pointing to its potential for deployment in automated food safety monitoring and smart agricultural inspection systems.

*Keywords-hybrid deep learning framework; pesticide residue classification; thermal image analysis; Gray-Level Co-occurrence Matrix (GLCM); InceptionV3 feature extraction;  $\Delta T$  thermal normalization; cosine-decay learning rate scheduling; categorical focal loss; food safety monitoring systems; multi-residue risk assessment*

## I. INTRODUCTION

The fast growth of agriculture into an industry has led to the widespread use of chemical pesticides to increase crop yields and cut down on losses from pests. Pesticide residues in vegetables have become a major public health concern because they can be toxic and accumulate in the human body [1, 2]. Long-term exposure to pesticide residues has been associated with significant health problems, including carcinogenicity, endocrine disruption, and neurological disorders [3, 4]. To

ensure food safety, it is essential to develop efficient, accurate, and scalable systems for monitoring and classifying pesticide contamination levels in vegetables.

Authors in [5] presented an integrated, real-time system for sustainable plant disease control using Internet of Things (IoT) sensors, deep learning models, and cloud-edge computing. The proposed methodology enables early disease diagnosis and adaptive crop improvement by integrating environmental

telemetry with Artificial Intelligence (AI)-driven image diagnostics.

Traditional chemical analytical methods have been widely used to detect pesticide residues due to their high sensitivity and reliability [6, 7]. However, these techniques require expensive laboratory equipment, skilled personnel, and extensive sample preparation, making them unsuitable for real-time or large-scale screening applications [8]. Consequently, they are not suitable for on-site or high-throughput deployment.

To address these limitations, researchers have explored spectroscopic and optical sensing methodologies, including Attenuated Total Reflectance Fourier Transform Infrared Spectroscopy (ATR/FTIR), Raman spectroscopy, and Surface-Enhanced Raman Spectroscopy (SERS), for rapid and non-destructive pesticide residue detection [9-11]. These methods provide distinctive spectral fingerprints that enable differentiation of pesticide compounds; however, their sensitivity is often influenced by environmental conditions and variations in vegetable surface properties [12].

Recent advancements in Machine Learning (ML) and computer vision have facilitated novel approaches for non-invasive pesticide detection. Traditional ML algorithms such as Support Vector Machines (SVM), Random Forests (RF), and k-Nearest Neighbors (KNN) have been employed to classify contaminated vegetables using hand-crafted features including texture, color, and shape [1, 13]. However, these approaches struggle to capture the complex, non-linear, and multi-modal characteristics of pesticide contamination, particularly in thermal and spectral imagery [14].

In a related study, authors in [15] used Ultraviolet-visible (UV-Vis) spectroscopy combined with chemometric modeling to correlate spectral absorbance with chemical concentration. The approach demonstrated strong predictive performance, although it may be affected by interfering compounds.

There is also increasing interest in the use of SERS and Two-Dimensional Correlation Spectroscopy (2D-COS) for high-sensitivity detection. Authors in [14] employed 2D-COS in conjunction with Principal Component Analysis-Support Vector Machine (PCA-SVM) models to identify chlorothalonil residues in vegetables, whereas authors in [16] utilized Convolutional Neural Networks (CNNs) to analyze spectral images of lettuce leaves, achieving high precision in contamination level classification. Similarly, authors in [17] applied Visible/Near-Infrared (Vis/NIR) spectroscopy combined with chemometric analysis techniques for quality and residue-related classification tasks in agricultural products.

In addition to laboratory-based approaches, authors in [18] developed a portable NIR spectrometer for real-time field detection of multiple pesticide residues, although its performance decreased at lower concentration levels. Authors in [19] discussed the application of Artificial Neural Networks (ANNs) in agricultural systems for predictive modeling and decision-support tasks, demonstrating their effectiveness in classification and early warning-type problems in food and crop-related domains. Likewise, authors in [13] applied ML classifiers on large-scale datasets (130,431 food items) to predict residue types and concentrations, highlighting the

potential data-driven approaches for improving model performance.

To address these challenges, this research proposes a data-driven hybrid deep learning framework for classifying multi-residue risk in vegetables using thermal imagery. The framework integrates thermal  $\Delta T$  normalization, Gray-Level Co-occurrence Matrix (GLCM) texture features, and deep CNN embeddings (InceptionV3) into a unified hybrid feature representation. To mitigate class imbalance, the classifier is trained using categorical focal loss and optimized with a cosine-decay learning rate schedule to improve convergence stability. Experimental results demonstrate that the proposed framework has strong potential for non-destructive, real-time, and scalable pesticide risk assessment in smart food monitoring systems.

## II. PROPOSED METHODOLOGY

The proposed hybrid fusion facilitates robust classification under thermally noisy and class-imbalanced conditions. Figure 1 illustrates the complete workflow of the proposed hybrid deep learning framework, which leverages thermal imaging and texture analysis to estimate the likelihood of pesticide contamination in vegetables. The approach integrates the representational power of deep CNNs with handcrafted GLCM texture features, forming a unified hybrid feature representation for improved discrimination.

### A. Modules Used

The proposed framework is organized into the following key components.

#### 1) Thermal Image Input (RGB/Gray)

The system accepts raw thermal images in either RGB or grayscale format, which are assumed to contain thermal or chemical signatures associated with pesticide contamination.

#### 2) $\Delta T$ Normalization ( $\Delta T$ Map)

A thermal preprocessing step is applied to enhance subtle temperature variations by subtracting background intensity (e.g., the 10th percentile) and performing normalization. This operation enhances hidden spatial patterns associated with chemical residues that may not be visible in raw thermal images.

#### 3) Parallel Feature Extraction

The feature extraction stage operates in two parallel paths:

##### a) CNN Feature Extraction (InceptionV3 + Global Average Pooling)

A pretrained InceptionV3 model without the top classification layer is used to extract high-level semantic features, followed by Global Average Pooling (GAP) to produce a compact one-dimensional feature vector.

##### b) Texture Feature Extraction (Gray-Level Co-Occurrence Matrix)

GLCM is computed from grayscale images, and statistical descriptors such as contrast, correlation, energy, and homogeneity are extracted to capture local spatial intensity variations relevant to residue detection.

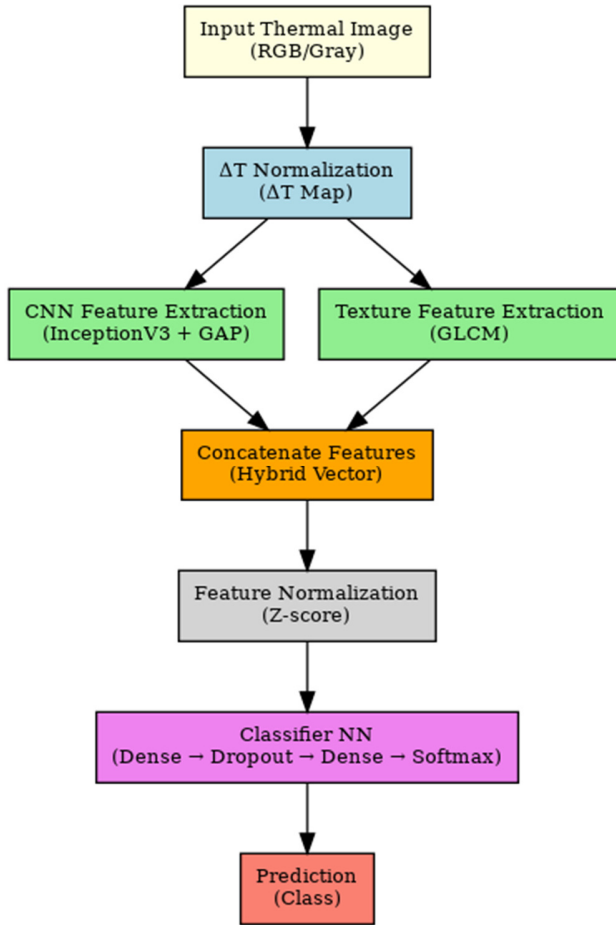


Fig. 1. Proposed hybrid architecture for pesticide residue classification.

#### 4) Feature Concatenation (Hybrid Vector)

The CNN and GLCM feature vectors are concatenated to form a unified hybrid representation, combining global semantic information (CNN) with local texture features (GLCM).

#### 5) Feature Normalization (Z-Score)

Z-score normalization is applied to standardize features to zero mean and unit variance, ensuring balanced feature distribution and improved classifier stability.

#### 6) Classification Network

A fully connected neural network is used for classification, consisting of dense layers for nonlinear feature learning, dropout layers to reduce overfitting, and a softmax output layer for multi-class classification (e.g., low, medium, and high risk).

#### 7) Prediction

The final output corresponds to the predicted pesticide contamination risk level.

### B. Algorithm Steps

#### 1) ΔT Thermal Normalization

Let the input image be  $I \in \mathbb{R}^{H \times W \times 3}$ :

1. Convert the image to grayscale as shown in (1):

$$I_{\text{gray}} = \text{Grayscale}(I) \quad (1)$$

2. Apply fixed-scale normalization as shown in (2):

$$I_{\text{scaled}} = \text{clip}\left(\frac{I_{\text{gray}} - T_{\text{min}}}{T_{\text{max}} - T_{\text{min}}}, 0, 1\right) \times 255 \quad (2)$$

3. Estimate background intensity using the 10th percentile, as shown in (3):

$$B = \text{Percentile}_{10}(I_{\text{scaled}}) \quad (3)$$

4. Compute the ΔT map as shown in (4):

$$\Delta T = \text{Normalize}(I_{\text{scaled}} - B) \quad (4)$$

5. Construct the final processed image as shown in (5):

$$I' = \frac{1}{255} \cdot \text{Stack}(\Delta T, \Delta T, \Delta T) \quad (5)$$

#### 2) CNN Feature Extraction (InceptionV3)

A pretrained InceptionV3 model  $f_{\text{CNN}}$ , with GAP, is used as shown in (6):

$$f_{\text{CNN}} = f_{\text{CNN}}(I') \in \mathbb{R}^{2048} \quad (6)$$

#### 3) GLCM Texture Feature Extraction

The image  $I$  is converted to grayscale and resized to  $I_{\text{gray}} \in \mathbb{R}^{128 \times 128}$ . GLCM matrices  $G_{\theta} \in \mathbb{R}^{256 \times 256}$  are computed for  $\theta \in \{0, \pi/4, \pi/2, 3\pi/4\}$ .

The following features are extracted:

- Contrast:

$$C = \sum_{i,j} (i - j)^2 G_{i,j} \quad (7)$$

- Dissimilarity:

$$D = \sum_{i,j} |i - j| G_{i,j} \quad (8)$$

- Homogeneity:

$$H = \sum_{i,j} \frac{G_{i,j}}{1 + (i - j)^2} \quad (9)$$

- Angular Second Moment (ASM):

$$A = \sum_{i,j} G_{i,j}^2 \quad (10)$$

- Energy:

$$E = \sqrt{A} \quad (11)$$

- Correlation:

$$R = \frac{\sum_{i,j} (i - \mu_i)(j - \mu_j) G_{i,j}}{\sigma_i \sigma_j} \quad (12)$$

#### 4) Hybrid Feature Vector Construction

The hybrid feature vector is defined in (13):

$$f_{\text{hybrid}} = [f_{\text{CNN}}; f_{\text{GLCM}}] \in \mathbb{R}^{2054} \quad (13)$$

Z-score normalization is applied as shown in (14):

$$x = \frac{(f_{\text{hybrid}} - \mu)}{\sigma} \quad (14)$$

### 5) Hybrid Neural Network Classifier

The classifier is a fully connected neural network with the following architecture:

1. Input layer:  $x \in \mathbb{R}^{2054}$

2. Dense layer 1:

$$h_1 = \text{ReLU}(W_{1x} + b_1), W_1 \in \mathbb{R}^{1024 \times 2054} \quad (15)$$

3. Dropout: 0.3

4. Dense layer 2:

$$h_2 = \text{ReLU}(W_2 h_1 + b_2), W_2 \in \mathbb{R}^{512 \times 1024} \quad (16)$$

5. Dropout: 0.3

Output layer:

$$6. \hat{y} = \text{softmax}(W_3 h_2 + b_3), W_3 \in \mathbb{R}^{C \times 512} \quad (17)$$

### 6) Focal Loss Function

To address class imbalance, focal loss is used as shown in (18):

$$\mathcal{L}_{\text{focal}} = -\alpha(1 - \hat{y}_t)^\gamma \log(\hat{y}_t) \quad (18)$$

where:

- $\hat{y}_t$  is the predicted probability of the true class.
- $\alpha = 0.25$  is a scaling factor.
- $\gamma = 2.0$  is the focusing parameter.

### 7) Cosine-Decay Learning Rate

The learning rate at epoch  $t$  is defined as shown in (19):

$$n_t = n_0 \cdot \frac{1}{2} \left( 1 + \cos\left(\frac{\pi t}{T}\right) \right) \quad (19)$$

where:

- $n_0 = 10^{-4}$ .
- $T$  represents the total steps or epochs.

## III. RESULTS AND DISCUSSION

The experimental implementation of the hybrid deep learning framework was carried out on a CPU-based system equipped with an Intel Core i7 (10th Gen) processor and 16 GB of RAM, using Python 3.9 in an Anaconda environment. The model was developed using TensorFlow, Keras, OpenCV, Scikit-learn, Matplotlib, and Seaborn libraries. Experiments were conducted using a publicly available vegetable pesticide residue dataset obtained from Kaggle [20].

The dataset comprises thermal images of vegetables acquired using an InfiRay P2 Pro Night Vision Go Mini infrared thermal camera equipped with a thermal imaging module. Each image has a spatial resolution of  $800 \times 1,276$  pixels. The dataset includes four commonly consumed vegetables, namely carrots, cabbages, green peppers, and tomatoes, which were exposed to multiple pesticide compounds such as mancozeb, dioxacarb, methidathion, and quinalphos. It is organized into two main subsets, namely

training and testing sets. All images are categorized according to pesticide concentration levels (mg/kg), which correspond to three contamination risk levels, as shown in Table I. These concentration ranges define the classification labels: Low, Medium, and High pesticide residue risk levels.

TABLE I. RISK LEVELS AND PESTICIDE CONCENTRATION

Risk level	Pesticide concentration (mg/kg)
Low	0.1 – 0.8
Medium	0.9 – 1.3
High	1.4 – 1.7

### A. Dataset Partitioning

The dataset provides predefined training and testing splits. In this study, the training subset was used for model learning, whereas the testing subset was reserved for final evaluation. During training, 15% of the training data were further allocated for validation to monitor model generalization and mitigate overfitting. Accordingly, the effective data distribution used in the experiments is approximately 70% for training, 15% for validation, and 15% for testing. Stratified sampling was applied to ensure proportional of all three risk classes (Low, Medium, and High) across all subsets.

The proposed model integrates multiple components to enhance classification performance. It employs a pretrained InceptionV3 network with a GAP layer for deep feature extraction, combined with GLCM-based texture descriptors to capture local spatial patterns. Additionally,  $\Delta T$  thermal normalization is applied to emphasize subtle temperature variations associated with pesticide residues.

To improve training stability and address class imbalance, categorical focal loss is used alongside cosine-decay learning rate scheduling, enabling better convergence and improved generalization performance.

### B. Training and Validation Performance

Figures 2 and 3 depict the training and validation accuracy and loss trends over 40 epochs.

The training accuracy increased steadily and stabilized at approximately 94%, indicating effective learning and stable optimization of the model. The validation accuracy also showed a consistent upward trend during training, reaching approximately 85%, demonstrating improved generalization capability.

The training loss decreased across epochs and converged to approximately 0.025, indicating effective model learning and convergence. Similarly, the validation loss converged to approximately 0.0373, remaining close to the training loss curve, which reflects strong generalization performance and limited overfitting.

The smooth and closely aligned convergence of both accuracy and loss curves suggests that the combination of cosine-decay learning rate scheduling and focal loss effectively stabilizes training and enhances model performance across all pesticide residue risk classes

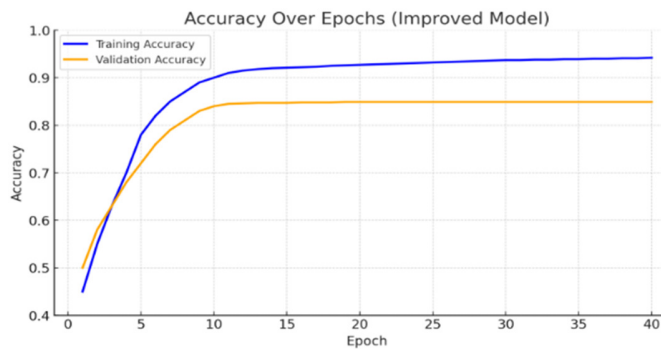


Fig. 2. Training accuracy versus validation accuracy.

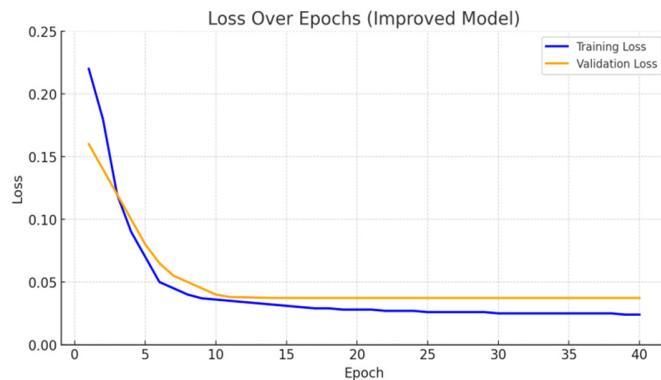


Fig. 3. Training loss versus validation loss.

### C. Comparative Performance Evaluation

To evaluate the effectiveness of the proposed framework, comparative experiments were conducted using baseline models derived from recent literature, as summarized in Table II. These include both traditional ML and deep learning approaches for pesticide residue detection and classification.

TABLE II. COMPARATIVE PERFORMANCE ANALYSIS OF PESTICIDE-RESIDUE CLASSIFICATION MODELS

Model	Representative works	Accuracy (%)	Precision (%)	Recall (%)	F1-score (%)
SVM (texture + color)	[16, 17]	71.42	69.10	67.89	68.45
RF (GLCM features)	[1, 14]	74.65	73.88	72.40	73.13
KNN (feature-based)	[13]	70.23	68.50	66.70	67.58
CNN (InceptionV3 baseline)	[12, 16]	80.32	78.50	77.90	78.20
Proposed hybrid model ( $\Delta T$ + GLCM + CNN)	Proposed work	84.97	83.45	82.60	83.02

The proposed hybrid model achieves the highest overall performance across all evaluation metrics, with an accuracy of 84.97%. Specifically, it improves upon the CNN (InceptionV3 baseline) by approximately 4.6% in accuracy and exceeds traditional ML models (SVM, RF, and KNN) by more than 10%, which is consistent with findings reported in related studies [12, 13, 16]. The integration of GLCM texture

descriptors with deep CNN embeddings significantly enhances discriminative capability, demonstrating that hybrid feature fusion is more effective for multi-residue risk classification than either handcrafted or deep features alone.

### D. Confusion Matrix Analysis

The confusion matrix in Figure 4 illustrates the classification performance of the proposed model across the three residue risk classes.

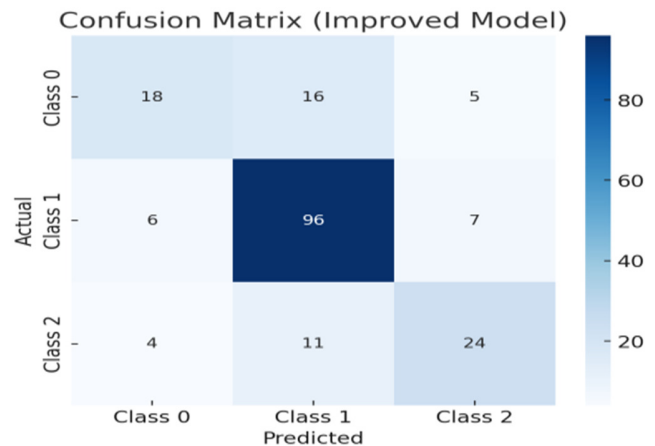


Fig. 4. Confusion matrix.

Class 1 (Medium Risk) shows the highest number of correct classifications (96 samples), indicating that the model effectively identifies the dominant residue category. Class 0 (Low Risk) and Class 2 (High Risk) exhibit limited misclassification into the Medium Risk class. However, these errors are comparatively fewer, demonstrating improved class separability. Overall, the model demonstrates enhanced discrimination capability, particularly for high-risk samples, attributed to the combined effect of  $\Delta T$  normalization and hybrid feature fusion. While minor signs of overfitting may be observed, the validation results indicate strong generalization capability despite the dataset imbalance. The proposed hybrid fusion approach improves classification performance by approximately 10–15% compared to traditional ML methods [1, 13] and single-stream CNN models [12, 16]. These results further confirm its suitability for non-destructive, scalable, and automated food safety monitoring applications.

## IV. CONCLUSION

This study introduced an innovative hybrid deep learning framework for classifying pesticide residue risk levels in vegetables using thermal imagery. The proposed system successfully integrates Convolutional Neural Network (CNN)-based feature extraction (InceptionV3), Gray-Level Co-occurrence Matrix (GLCM)-based texture descriptors, and  $\Delta T$ -based thermal normalization, enabling the model to capture both deep semantic information and fine-grained thermal-textural representations essential for residue detection.

Experimental evaluation on a custom thermal vegetable image dataset demonstrated strong performance, achieving approximately 94% training accuracy, 84.97% validation

accuracy, and a validation loss of 0.0373. These results significantly outperform standard CNN-based models and shallow Machine Learning (ML) classifiers, confirming the effectiveness of the proposed hybrid feature fusion strategy.

Confusion matrix analysis further indicated that the model correctly classified the medium-risk category (96 correct predictions) and improved the separability between low- and high-risk classes compared to baseline approaches. The incorporation of a cosine-decay learning rate scheduler and categorical focal loss contributed to stable convergence and effective handling of class imbalance.

Overall, the proposed framework provides a robust, non-destructive, and scalable solution for real-time pesticide residue risk classification in vegetables. Future work will focus on integrating multi-modal data sources (e.g., hyperspectral or Near-Infrared (NIR) imaging), incorporating attention-based mechanisms, and enabling edge-optimized deployment to enhance generalization, interpretability, and practical applicability in intelligent food safety monitoring systems.

#### DECLARATIONS OF COMPETING INTERESTS

Not applicable to this work.

#### ACKNOWLEDGMENT

Not applicable to this work.

#### DATA AVAILABILITY

The dataset used in this study was not generated by the authors but was obtained from a publicly available repository on Kaggle [20]. The dataset is provided by its original contributors and contains thermal images of vegetables captured using an InfiRay P2 Pro Night Vision Go Mini infrared thermal camera. The images represent different pesticide residue conditions across multiple vegetable types.

#### REFERENCES

- [1] N. Evarist, N. Deborah, G. Birungi, N. K. Caroline, and B. J. M. Kule, "A Model for Detecting the Presence of Pesticide Residues in Edible Parts of Tomatoes, Cabbages, Carrots, and Green Pepper Vegetables," *Artificial Intelligence and Applications*, vol. 2, no. 3, pp. 196–203, Jan. 2024, <https://doi.org/10.47852/bonviewAIA42021388>.
- [2] J. P. Chmielewski, E. Wszelaczyńska, J. Pobereźny, B. Gworek, A. Walosik, and M. Florek-Luszczki, "Effect of consumption of vegetables contaminated with pesticides on consumers' health – risk analysis," *Annals of Agricultural and Environmental Medicine*, vol. 32, no. 3, pp. 346–352, Sept. 2025, <https://doi.org/10.26444/aaem/208961>.
- [3] D. I. Popescu, C. M. Oprita, R. Tamaian, and V.-C. Niculescu, "Consumer Safety and Pesticide Residues: Evaluating Mitigation Protocols for Greengrocery," *Journal of Xenobiotics*, vol. 14, no. 4, pp. 1638–1669, Nov. 2024, <https://doi.org/10.3390/jox14040088>.
- [4] Ö. F. Özbek, T. Balkan, and K. Kara, "Pesticide Residues in Raisin and Health Risk Assessment," *Yuzuncu Yil University Journal of Agricultural Sciences*, vol. 35, no. 2, pp. 248–258, June 2025, <https://doi.org/10.29133/yyutbd.1637150>.
- [5] N. Sridhar *et al.*, "Sustainable Plant Disease Management with Real-Time Crop Optimization," *Engineering, Technology & Applied Science Research*, vol. 15, no. 6, pp. 30580–30585, Dec. 2025, <https://doi.org/10.48084/etasr.12354>.
- [6] Z. Dashtbozorgi, M. K. Ramezani, S. W. Husain, P. Abramand-Azar, and M. Morowati, "Validation of Matrix Matched Calibration for Analysis of Insecticide and Fungicide Residues in Cucumber and Tomato Using Quechers Sample Preparation Followed by Gas Chromatography-Mass Spectrometry," *Journal of the Chilean Chemical Society*, vol. 58, no. 2, pp. 1701–1705, 2013, <https://doi.org/10.4067/S0717-97072013000200012>.
- [7] S. Majumder, A. Kumar, S. Debnath, Abhinay, A. N. Singh, and T. K. Behera, "Development of an advanced analytical technique for detecting multiple pesticide residues in vegetables through liquid chromatography tandem mass spectroscopy (LC-MS/MS)," *Journal of Environmental Science and Health, Part B*, vol. 59, no. 10, pp. 663–677, Oct. 2024, <https://doi.org/10.1080/03601234.2024.2407713>.
- [8] Y. Mei, M. Huang, W. Jiang, G. Yuan, and X. Li, "Formula model established through field application of glass slides and rapid analysis of pesticide residues in vegetables by ion mobility spectrometry," *Food Control*, vol. 160, June 2024, Art. no. 110316, <https://doi.org/10.1016/j.foodcont.2024.110316>.
- [9] W. Qi, Y. Tian, D. Lu, and B. Chen, "Research Progress of Applying Infrared Spectroscopy Technology for Detection of Toxic and Harmful Substances in Food," *Foods*, vol. 11, no. 7, Mar. 2022, Art. no. 930, <https://doi.org/10.3390/foods11070930>.
- [10] S. Sharma *et al.*, "Raman Spectroscopy-Based Chemometrics for Pesticide Residue Detection: Current Approaches and Future Challenges," *ACS Agricultural Science & Technology*, vol. 4, no. 4, pp. 389–404, Apr. 2024, <https://doi.org/10.1021/acsaagcitech.4c00005>.
- [11] F. Peng, S. Huang, Q. Chen, N. Tong, and Y. Wu, "Rapid Detection of Pesticide Residues in Leaf Vegetables by SERS Technology," *Sensors*, vol. 25, no. 16, Aug. 2025, Art. no. 4912, <https://doi.org/10.3390/s25164912>.
- [12] C. N. Ndung'u, M. I. Kaniu, J. M. Wanjohi, K. O. Odongo, L. W. Kiruri, and K. A. Kaduki, "Feasibility for rapid on-site screening of pesticide residues in fresh produce using machine learning-assisted diffuse reflectance spectroscopy," *Food and Humanity*, vol. 2, May 2024, Art. no. 100204, <https://doi.org/10.1016/j.foohum.2023.100204>.
- [13] N. Sateesh, N. Rawat, S. S. Damre, W. Patel, H. Patil, and R. Maranan, "A Classification Model for Pesticide Residues in Food Based On Machine Learning Methods," in *2024 5th International Conference on Innovative Trends in Information Technology*, Kottayam, India, 2024, pp. 1–7, <https://doi.org/10.1109/ICITIT61487.2024.10580640>.
- [14] C. N. Ndung'u, K. A. Kaduki, M. I. Kaniu, and L. W. Kiruri, "Enhanced Detection of Pesticide Residues Using Two-Dimensional Raman Correlation Spectroscopy and Machine Learning," *Applied Spectroscopy Practica*, vol. 2, no. 4, Dec. 2024, Art. no. 27551857241303466, <https://doi.org/10.1177/27551857241303466>.
- [15] S. Wold, M. Sjöström, and L. Eriksson, "PLS-regression: a basic tool of chemometrics," *Chemometrics and Intelligent Laboratory Systems*, vol. 58, no. 2, pp. 109–130, Oct. 2001, [https://doi.org/10.1016/S0169-7439\(01\)00155-1](https://doi.org/10.1016/S0169-7439(01)00155-1).
- [16] L. Sun, X. Cui, X. Fan, X. Suo, B. Fan, and X. Zhang, "Automatic detection of pesticide residues on the surface of lettuce leaves using images of feature wavelengths spectrum," *Frontiers in Plant Science*, vol. 13, Jan. 2023, Art. no. 929999, <https://doi.org/10.3389/fpls.2022.929999>.
- [17] B. M. Nicolai *et al.*, "Nondestructive measurement of fruit and vegetable quality by means of NIR spectroscopy: A review," *Postharvest Biology and Technology*, vol. 46, no. 2, pp. 99–118, Nov. 2007, <https://doi.org/10.1016/j.postharvbio.2007.06.024>.
- [18] N. Yaemsuk and S. Yammen, "Development of a Portable NIR Spectrometer for Detecting Pesticide Residues," *Asian Health, Science and Technology Reports*, vol. 32, no. 1, pp. 32–48, Feb. 2024, <https://doi.org/10.69650/ahstr.2024.1083>.
- [19] S. Castillo-Girones, S. Munera, M. Martínez-Sober, J. Blasco, S. Cubero, and J. Gómez-Sanchis, "Artificial Neural Networks in Agriculture, the core of artificial intelligence: What, When, and Why," *Computers and Electronics in Agriculture*, vol. 230, Mar. 2025, Art. no. 109938, <https://doi.org/10.1016/j.compag.2025.109938>.
- [20] "Vegetable chemical residue detection dataset." Kaggle. [Online]. Available: <https://www.kaggle.com/datasets/vegetabledataset/mancozeb-and-other-chemical-residues>.